Structure
Article

Specific Inhibition of Caspase-3 by a Competitive DARPin: Molecular Mimicry between Native and Designed Inhibitors

Thilo Schroeder,[1,2] Jonas Barandun,[1,2,3] Andreas Flütsch,[1,2] Christophe Briand,[1] Peer R.E. Mittl,[1] and Markus G. Grütter[1,*]
[1]Department of Biochemistry, University of Zurich, Winterthurerstrasse 190, CH-8057 Zürich, Switzerland
[2]These authors contributed equally to this work
[3]Present address: Institute of Molecular Biology and Biophysics, Schafmattstrasse 20, ETH Zürich, CH-8093 Zürich, Switzerland
*Correspondence: gruetter@bioc.uzh.ch
http://dx.doi.org/10.1016/j.str.2012.12.011

SUMMARY

Dysregulation of apoptosis is associated with several human diseases. The main apoptotic mediators are caspases, which propagate death signals to downstream targets. Executioner caspase-3 is responsible for the majority of cleavage events and its therapeutic potential is of high interest with to date several available active site peptide inhibitors. These molecules inhibit caspase-3, but also homologous caspases. Here, we describe caspase-3 specific inhibitors D3.4 and D3.8, which have been selected from a library of designed ankyrin repeat proteins (DARPins). The crystal structures of D3.4 and mutants thereof show how high specificity and inhibition is achieved. They also show similarities in the binding mode with that of the natural caspase inhibitor XIAP (X-linked inhibitor of apoptosis). The kinetic data reveal a competitive inhibition mechanism. D3.4 is specific for caspase-3 and does not bind the highly homologous caspase-7. D3.4 therefore is an excellent tool to define the precise role of caspase-3 in the various apoptotic pathways.

INTRODUCTION

Apoptosis is a central process for the development and tissue homeostasis of multicellular organisms. It is characterized by morphological changes such as nuclear fragmentation, membrane blebbing, or the formation of apoptotic bodies (Wyllie et al., 1980). In multicellular organisms including humans, improper regulation of apoptosis leads to a variety of pathologies such as cancer, autoimmune diseases, and neurodegenerative disorders (Riedl and Shi, 2004). Apoptosis is triggered by various internal and external stimuli, which are propagated by different pathways. Common to all apoptotic pathways are caspases (Fuentes-Prior and Salvesen, 2004; Grütter, 2000; Riedl and Shi, 2004). These proteins are synthesized as inactive proenzymes and activated upon triggering of the cell death machinery: The activation of initiator caspases occurs through dimerization (induced proximity model; Boatright et al., 2003; Muzio et al., 1998), followed by autoproteolytic cleavage of the prodomain and the linker between the two subdomains. Executioner caspases exist as dimeric zymogens and are activated by proteolytic cleavage of the N-terminal pro-peptide and the intersubunit linker (Fuentes-Prior and Salvesen, 2004). Active caspases are dimers of two catalytic domains with a small p10 and a large p20 chain.

Of the 11 known human caspases, caspase-3 plays a prominent role in the apoptotic cascade. Caspase-3 is activated by intrinsic and/or extrinsic death signals and it executes cell death by the cleavage of downstream key mediators of apoptosis (Timmer and Salvesen, 2007). Because apoptosis is a dangerous process for the cell, caspase activation is strictly controlled and all apoptotic signaling pathways are tightly regulated. All caspases recognize tetrapeptide sequences, which are characterized by an aspartic acid at the C terminus (P1 position) and either tryptophan, aspartic acid or leucine residues at the N terminus (P4 position) conferring selectivity for caspase-1, -3, and -8, respectively. The P4 selectivity has been attributed to different interactions with residues in loops flanking the P4 binding pocket (Mittl et al., 1997; Rotonda et al., 1996). However, the selectivity of short peptidic substrates remains controversial. It has been reported that the in vitro selectivity of caspase-3 for a substrate harboring a P4 aspartic acid is at least 100-fold higher than that for a glutamate or an asparagine (Stennicke et al., 2000). Despite this finding, commercially available peptide substrates failed to exhibit the expected caspase selectivity (McStay et al., 2008). Caspase-3 is the most unrestrained and efficient caspase and it is often more active in cleaving short peptide substrates than the caspase for which the peptide substrate was designed for (McStay et al., 2008). This analysis raised doubt regarding the use of short peptides to dissect signaling cascades leading to apoptosis. The observation that naturally occurring caspase inhibitors, such as X-linked inhibitor of apoptosis (XIAP), are highly specific for caspase-3 and -7 (Deveraux et al., 1997; Roy et al., 1997) suggests that specificity can be gained by extending the size of the inhibitor. Caspases are attractive drug targets because they are implicated in various diseases. Therefore, selective and potent caspase-specific inhibitors are highly desirable.

To develop a caspase-3 specific inhibitor, we used the Designed Ankyrin Repeat Protein (DARPin) technology (Binz et al., 2003). From a highly diverse library of DARPin molecules, binders that recognize the target molecule can be selected by

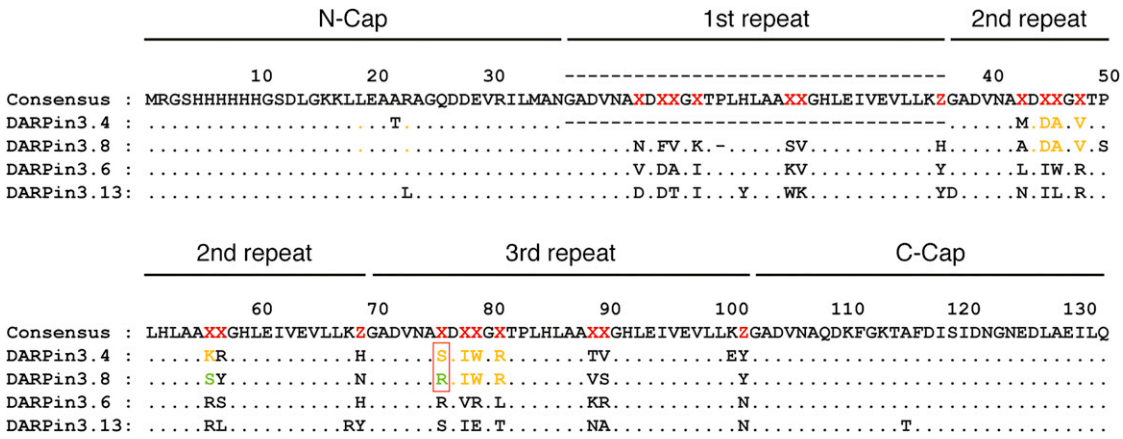

Figure 1. Sequence Alignment of Caspase-3-Specific DARPin Binders

The general DARPin sequence is shown with the consensus sequence in black and the randomized amino acid positions in red (X, any of the 20 natural amino acids except cysteine, glycine, or proline; Z, any of the amino acids asparagine, histidine, or tyrosine). Four DARPin sequences are aligned to the consensus sequence with identical residues represented as a dot. Amino acids involved in the interaction with caspase-3 are colored in orange. Differences among the D3.4 and D3.8 sequences are highlighted in green. The D3.4_S76R mutation is marked by a red box. The sequence number is based on D3.4, a N2C DARPin that lacks the first internal repeat.

either ribosome- or phage display (Steiner et al., 2006; Zahnd et al., 2007). DARPins consist of N- and C-terminal capping repeats and two or three internal repeats. These internal repeats recognize the target molecule by means of specific amino acids that are randomized in the DARPin library. DARPins possess several beneficial properties that make them attractive for biotechnological applications. They are thermodynamically stable, easily produced, and do not contain cysteine residues allowing intracellular applications (Binz et al., 2005). Highly selective DARPins have been successfully selected and described for a variety of different target proteins such as caspase-2 (Schweizer et al., 2007) or kinase inhibitors (Amstutz et al., 2005), crystallization chaperones (Sennhauser et al., 2007), HIV inhibitors (Schweizer et al., 2008), and tumor-targeting binding molecules (Zahnd et al., 2010).

Here, we report the selection and characterization of DARPins that bind to active caspase-3. Kinetic and binding experiments revealed that DARPins D3.4 and D3.8 are competitive caspase-3 inhibitors that do not recognize other members of the caspase family at all (D3.4) or only extremely weakly caspase-7 (D3.8). The structure of the caspase-3/D3.4 complex reveals the critical interactions leading to high specificity and tight binding and analogies to XIAP inhibition.

RESULTS

Selection of Caspase-3-Specific DARPin Binders

A DNA library containing NI_2C and NI_3C DARPins was used to select caspase-3 binders by ribosome display (Zahnd et al., 2007). After four selection rounds, 768 putative binders were screened by crude cell extract ELISA yielding 29 clones that possessed submicromolar affinities for caspase-3. These high affinity binders were individually expressed, purified, and their binding affinities for caspase-3 were determined by surface plasmon resonance (SPR) analysis. Four of the selected DARPins showed affinities below 10 nM (Figure S1 available online). Their sequences were aligned and are shown in Figure 1. Although DARPins D3.4 and D3.8 contain 2 and 3 internal repeats, respectively, they possess the highest sequence similarity. Of the 14 randomized positions of the internal repeats seven residues are identical. When comparing the sequences of DARPin D3.6 and D3.13 only four residues in a total of 21 randomized positions are identical. Despite the different numbers of internal repeats all four DARPins possess very high affinities for caspase-3. SPR analysis revealed that D3.4, D3.6, D3.8 and D3.13 bind caspase-3 with K_D values of 9.6 ± 1.1 nM, 8.8 ± 2.0 nM, 3.4 ± 0.4 nM, and 7.7 ± 0.4 nM, respectively (Table 1). These K_D values were determined based on equilibrium analyses of the SPR signal. We used the heterogeneous ligand model to determine the kinetic values (Table 1), which suggests two epitopes with substantially different binding affinities (Morton et al., 1995).

Inhibition of Caspase-3 by DARPins D3.4 and D3.8

The inhibitory properties of the purified DARPins were analyzed using two different approaches. Initially the ability of the DARPins to inhibit the hydrolysis of the short chromogenic caspase-3 substrate Ac-DEVD-AMC was measured. These initial tests revealed that D3.4 and D3.8 inhibit the hydrolysis of the standard caspase-3 substrate with K_i values of 16.8 ± 0.3 nM and 6.7 ± 0.2 nM, respectively, whereas D3.6 and D3.13 showed no detectable inhibitory activities (Table 1). To characterize the mode of inhibition (competitive versus uncompetitive), specific velocity plot (Figure S2; Baici, 1981) analysis was performed, which yields the ratio between competitive and uncompetitive inhibitor constants (α) and the turnover rate of free enzyme to inhibited enzyme (β). For both DARPins we determined equal values of $\alpha = \infty$ and $\beta = 0$, demonstrating that D3.4 and D3.8 are purely competitive inhibitors of caspase-3 (Table 1).

In the past, short peptide substrates have been extensively used for the characterization of proteases, because the

Table 1. Kinetic Constants and Characteristics of the Interaction

	Kinetic					
DARPin	$k_{on1}(M^{-1s-1})$	$k_{off1}(s^{-1})$	$K_{D1}(M)$	$k_{on2}(M^{-1s-1})$	$k_{off2}(s^{-1})$	$K_{D2}(M)$
D3.4	2.85×10^5	8.81×10^{-3}	3.09×10^{-8}	1.12×10^6	1.13×10^{-3}	1.01×10^{-9}
D3.4_S76R	1.74×10^5	4.20×10^{-3}	2.42×10^{-8}	1.62×10^6	7.45×10^{-4}	4.61×10^{-10}
D3.6	1.48×10^5	1.13×10^{-3}	7.63×10^{-9}	1.46×10^6	1.00×10^{-2}	6.88×10^{-9}
D3.8	1.77×10^5	2.49×10^{-3}	1.41×10^{-8}	2.44×10^6	1.11×10^{-4}	4.57×10^{-11}
D3.13	2.74×10^5	1.24×10^{-3}	4.51×10^{-9}	2.31×10^6	7.86×10^{-3}	3.41×10^{-9}

	Equlibrium	Inhibition			Interaction		
DARPin	K_D(nM)	K_I(nM)	α	β	SC	Å^2	Δ^iG kcal/mol
D3.4	9.6 ± 1.1	16.8	∞	0	0.740	875.95	−6.1
D3.4_S76R	6.0 ± 0.5	3.5	∞	0	0.725	907.55	−7.1
D3.6	8.8 ± 2.0	–	–	–	–	–	–
D3.8	3.4 ± 0.4	6.7	∞	0	nd	nd	nd
D3.13	7.7 ± 0.4	–	–	–	–	–	–

See also Figures S1 and S2. nd, not determined.

determination of rate constants is straightforward in those experiments. On the other hand, short peptide substrates represent a rather artificial situation because these substrates utilize a very limited number of binding interactions. Natural protease substrates are significantly larger and consequently their binding is guided by a broader set of interactions. Therefore, we tested whether the selected DARPins also inhibit the processing of PARP-1, one of the best-characterized caspase-3 substrates. The 116-kDa PARP-1 is specifically cleaved by caspases-3 and -7 on the C-terminal side of Asp216 into an 85-kDa and a 31-kDa fragment (Lazebnik et al., 1994). The addition of 10-fold molar excess of D3.4 or D3.8 over caspase-3 inhibited the cleavage of PARP-1 by ~90%, whereas the addition of E3_5, a DARPin that does not bind caspase-3, showed no effect on the cleavage of PARP-1 (Figure 2). In addition, a 50-fold molar excess of the caspase-3 DARPin inhibitors completely abolishes PARP-1 cleavage (Figure 2).

Specificity of DARPins D3.4 and D3.8

All commercially available caspase inhibitors are capable of inhibiting both caspases-3 and -7 equally well (McStay et al., 2008). We investigated the caspase selectivity of D3.4 and D3.8 by measuring the binding affinity and inhibitory activity against caspase-7 (56% sequence identity with caspase-3) and the more distantly related caspase-6 (41% sequence identity). SPR analysis did not show any detectable binding of the caspase-3 directed DARPins D3.4 and D3.8 to caspases-6 or -7 (Figure S3), suggesting that both DARPins are highly specific for caspase-3. These results are consistent with the activity measurements where D3.4 and D3.8 were also unable to inhibit PARP-1 cleavage by caspase-7 (Figure 2). Probing the ability of D3.4 and D3.8 to inhibit the hydrolysis of chromogenic tetrapeptide substrates by caspases-1, -2, -4, -5, -6, -7, -8, and -9 revealed that D3.4 is highly specific for caspase-3 and cannot inhibit any other tested caspase, whereas D3.8 has a moderate inhibitory activity against caspase-7 (Figures 3 and S4). A 1,000-fold excess of D3.8 decreases the activity of caspase-7 to approximately 40%.

Crystal Structure Analysis of the Caspase-3/DARPin D3.4 Complex

To understand the structural basis for the inhibition mechanism of caspase-3 by DARPins the crystal structure of the caspase-3/D3.4 complex was determined at 2.1 Å resolution. The details of the structure determination (data collection and refinement) are listed in Table 2. In the crystal structure the asymmetric unit contains one $(p12, p17)_2$ caspase-3 heterotetramer and two D3.4 molecules (Figure 4A). In the complex every DARPin buries a surface area of 876 Å^2. A surface complementarity index of 0.74 indicates a good fit between D3.4 and caspase-3 (Table 1). The interface involves residues from the N-terminal capping repeat and the two internal repeats of the DARPin, which form specific hydrogen bonds and hydrophobic interactions with the caspase (Figure 4A). The crystal structure reveals first of all that D3.4 binds in the active site pocket of caspase-3 and prevents substrate molecules from accessing the catalytic residues (Figure 4A). The β-turns of D3.4 point toward the β strand of caspase-3 that is responsible for the recognition of the substrate by main chain hydrogen bonds (residues 205 to 207). This observation agrees very well with the kinetic analysis of the inhibition mechanism, where no uncompetitive contribution was observed ($\alpha = \infty$). Therefore, structural and kinetic analyses consistently classify D3.4 as a purely competitive caspase-3 inhibitor (Figure S2).

When comparing the caspase-3/D3.4 complex with previously published caspase/protein complexes, such as the caspase-2/AR_F8 (Schweizer et al., 2007) or the natural caspase-3/XIAP complexes (Riedl et al., 2001), the following features can be highlighted: (1) DARPins AR_F8 and D3.4 both bind to loop-4 (also termed 381-loop). However, AR_F8 binds from the backside and inhibits caspase-2 by an allosteric mechanism (Figure 4B). (2) D3.4 and XIAP are competitive caspase-3 inhibitors, but the main chains of D3.4 and the N-terminal extension loop of XIAP run in opposite directions (Figure 4C).

The binding mode of D3.4 shows similarities to the binding of natural substrates (based on inhibitor structures) and the natural inhibitor XIAP. Asp45 of D3.4 is located in the β-turn that

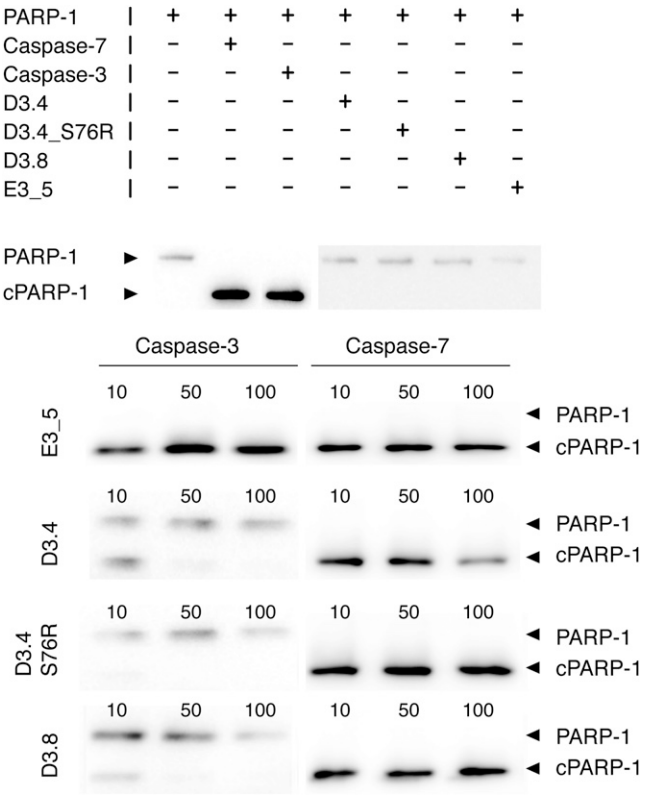

Figure 2. Inhibition of Caspase-3-Dependent PARP-1 Cleavage by DARPin Inhibitors

The cleavage of PARP-1 by caspase-3 (40 nM) and -7 (150 nM) was analyzed by SDS-PAGE (upper panel). Full length and cleaved PARP-1 (cPARP-1) were detected by a specific antibody that recognizes both forms. None of the selected DARPins cleave PARP-1 themselves. DARPins were added at 10-, 50-, and 100-fold molar excess per active site (lower panel).

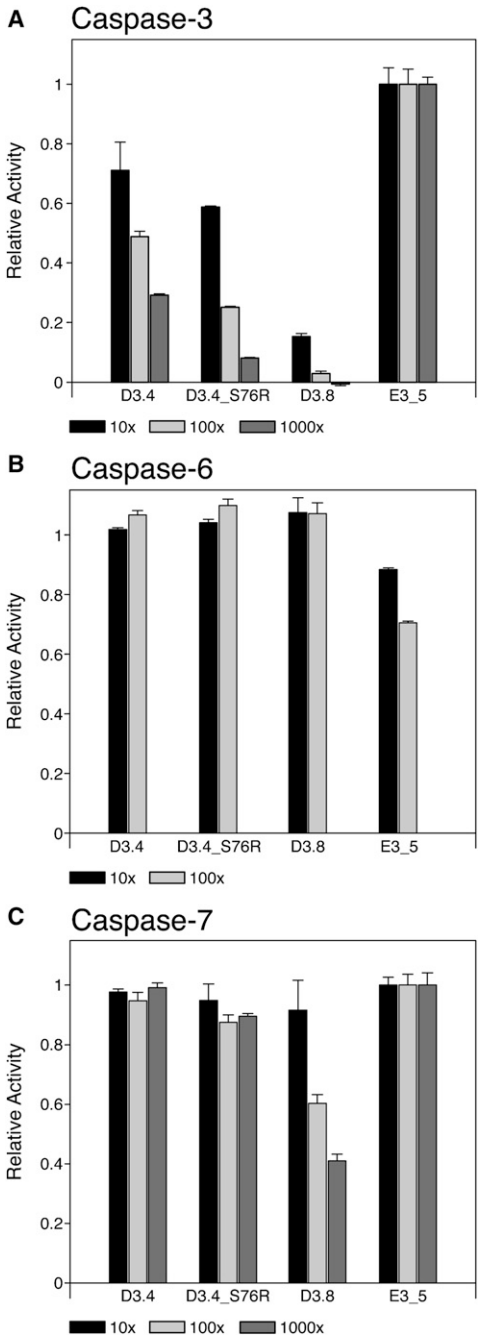

Figure 3. Specificity and Inhibition of Selected DARPins for Caspase-3, -6, and -7

(A–C) The relative enzymatic activity of caspase-3 is shown in the presence of D3.4, D3.4_S76R, D3.8, and E3_5 (control DARPin). Each DARPin was added at three different concentrations: 10- (black), 100- (light gray), and 1,000-fold molar excess (gray). All DARPins inhibit the activity of caspase-3 with the exception of E3_5. Shown are the relative enzymatic activities of caspase-6 (B) and −7 (C) in presence of four DARPins as described above. The 1000-fold molar excess of DARPin was not measured for caspase-6 because no inhibition was observed at 100-fold molar excess. D3.8 shows a moderate inhibition of caspase-7; all other DARPins are specific for caspase-3. Error bars represent the standard deviation of three independent experiments.

See also Figures S3 and S4.

connects the N-terminal capping repeat and the first internal repeat of D3.4, and its side chain occupies the S4 pocket of caspase-3 (Figure 5A). It forms a direct hydrogen bond with Asn208-ND2 and two water-mediated hydrogen bonds with Trp214-NE1 and Phe250-N (Figures 5A and S5). The main chain carbonyl oxygen of Asp45 forms another water-mediated (Wat10) hydrogen bond with Arg207-N of caspase-3. In other caspase-3 structures Arg207-N participates in an antiparallel β sheet with the substrate main chain. A water molecule (water 10) forms a third hydrogen bond with the hydroxyl group of-Tyr204. As a consequence, Thr166 moves toward the active site pocket and forms hydrogen bonds with Trp79-NE1 and Lys111-NZ from D3.4 (Figures 5A and 6A).

The tip of loop-4 of caspase-3 is recognized by the concave surface of D3.4 (Figures 5B and 5C). The side chain of Asp44 of D3.4 is buried in the interface and forms two hydrogen bonds with Ser251-OG and Phe252-N. In contrast, the side chains of Lys56 and Arg81 of D3.4 are solvent exposed and form salt bridges with the Asp253 side chain of caspase-3. Hydrophobic interactions seem to play equally important roles. The side chain of Phe256 of caspase-3 fits into a pocket that is formed by Ala46, Val48, Ile78, and Trp79 of D3.4. The benzyl ring of Phe256 of caspase-3 forms T-stacking interactions with the indole ring of D3.4

Table 2. X-Ray Data Collection and Model Refinement Statistics

	Caspase-3/ D3.4 (2XZD)	Caspase-3/ D3.4_S76R (2Y0B)
Data Collection		
Frame width (°)	0.25	0.2
Space group	$P3_121$	$P3_121$
Unit cell parameter	a = 98 Å	a = 98 Å
	b = 98.0 Å	b = 98.0 Å
	c = 193.6 Å	c = 192.9 Å
	$\alpha = \beta = 90.0°$ $\gamma = 120.0°$	$\alpha = \beta = 90.0°$ $\gamma = 120.0°$
Resolution (Å)	49.0–2.1	49.0–2.1
Wavelength (Å)	1.000	0.92
R_{sym} (%)	4.2 (60.4)	4.9 (60.9)
Completeness (%)	99.3 (99.5)	99.2 (99.5)
$I/\sigma(I)$	15.59 (1.92)	12.94 (1.96)
Refinement		
Resolution (Å)	2.1	2.1
R_F/R_{free} (%)	18.5/21.8	19.1/21.7
No. of protein atoms	5,616	5,622
No. of water atoms	247	345
Average B-factor ($Å^2$)	35.3	35.8
Root Mean Square Deviations		
Bond length (Å)	0.011	0.006
Bond angles (°)	1.192	0.941

Trp79 (Figure 5C). Although the Phe256 binding pocket is mainly hydrophobic, the side chain of Asp77 is located at the bottom of this pocket and forms an intramolecular salt bridge with Arg81 and a hydrogen bond with Wat26 (Figure 5C).

Comparison of the Caspase-3/D3.4 Structure with Caspase-3 in Complex with XIAP and DEVD

The overall structure of caspase-3 is identical to several other caspase structures. Superposition of the caspase-3/D3.4 structure with the caspase-3/z-DEVD-cmk (2DKO; Ganesan et al., 2006) and the caspase-3/XIAP complex structures (1I3O; Riedl et al., 2001) reveals rmsd values of 0.39 Å and 0.35 Å, respectively. Differences between caspase-3/D3.4 and the caspase-3/z-DEVD-cmk structures are observed in the active site pocket. In the caspase-3/D3.4 structure loop-4 of caspase-3 has moved approximately 1 Å out of the active site, whereas Thr166 has moved into the active site compared to the caspase-3/z-DEVD-cmk structure (Figure 6A). The movement of Thr166 is a consequence of the 120° rotation of the Tyr204 side chain. In the caspase-3/z-DEVD-cmk structure Tyr204 points toward Thr166, whereas in the caspase-3/D3.4 complex the Tyr204 side chain occupies the S2 pocket (Figure 6A).

The conformations of Tyr204 and loop-4 in the caspase-3/D3.4 complex structure resemble the conformations seen in the caspase-3/XIAP structure (1I3O) (Figure 6B). In both complexes, Tyr204 occupies the S2 pocket (Riedl et al., 2001). Furthermore, Tyr204 rests against a hydrophobic patch of the inhibitor, which is formed by Leu141 and Val146 in XIAP and by Ala46 and Ile78 in D3.4 (Figure 6B).

Modeling the Caspase-3/D3.8 Complex Structure

Based on the sequence alignment and the competitive inhibition we assume that D3.4 and D3.8 bind to the same epitope with similar interactions. We were not able to crystallize the caspase-3/D3.8 complex and thus calculated a homology model of D3.8 based on a N3C DARPin E3_5 structure (1MJ0; Kohl et al., 2003). This homology model was superimposed on D3.4 in the caspase-3/D3.4 crystal structure (Figure 6C). The N2C DARPin D3.4 lacks the first internal repeat so that the N-cap of D3.4 superimposes on the first internal repeat of the N3C DARPin D3.8 (Figure 6C). Furthermore, D3.8 has two critical mutations compared to D3.4. Mutations Lys56Ser and Ser76Arg are located in the caspase/DARPin interface, whereas all other amino acid changes between D3.4 and D3.8 are located more than 4 Å away from caspase-3. The homology model showed that the salt bridge between Lys56 and Asp253 is absent in the D3.8/caspase-3 complex (Figure 6D). In D3.8 the corresponding Ser56 is unable to form a salt bridge as observed in the caspase-3/D3.4 structure. Furthermore, the positive charge of Lys56 in D3.4 could cause repulsive interactions with His255 at the top of loop-4 of caspase-7 (Figure 6D). These repulsive interactions could explain why D3.4 does not show any affinity for caspase-7, whereas D3.8 possesses weak affinity for caspase-7 due to the Lys56Ser mutation.

D3.4 Mutant Ser76Arg

D3.8 binds caspase-3 with higher affinity and has a lower inhibition constant (K_i = 6.7 nM) compared to D3.4 (Table 1). Residue Ser76 in D3.4 is located in proximity to the interface but does not interact with caspase-3. The caspase-3/D3.8 model suggests that a bulkier side chain, such as arginine, could participate in an extended DARPin/caspase-3 interface. To test this hypothesis we generated the D3.4 Ser76Arg mutant (D3.4_S76R) and characterized its functional and structural properties. D3.4_S76R revealed dissociation and inhibitory constants of K_D^{S76R} = 6.0 ± 0.5 nM and K_i^{S76R} = 3.49 ± 0.03 nM, respectively. Thus, D3.4_S76R shows an equally low inhibitory constant for caspase-3 compared to D3.8 (Table 1).

The 2.1 Å resolution crystal structure of the caspase-3/D3.4_S76R complex revealed that although the overall structure is identical to the caspase-3/D3.4 structure (rmsd of 0.198 Å), the C-terminal capping repeat has shifted by approximately 2 Å (Figure 6E). The side chain of the newly introduced Arg76 forms two intramolecular hydrogen bonds with Gly80-O and Gln109-O of the C-terminal capping repeat and an intermolecular hydrogen bond with Gly60-O of caspase-3 (Figure 6E). In addition, the weak hydrogen bond between Lys111 and Thr166 as it is seen in the parent structure is broken and the Lys111 side chain points into the active site forming a water-mediated hydrogen bond with Gly165-O of caspase-3 and an intramolecular hydrogen bond with Ile78-O from the preceding DARPin repeat. The mediating water molecule is located in direct vicinity of the active site Cys163 (Figure 6E).

DISCUSSION

The development of specific caspase inhibitors has remained a challenging task due to the similarity between the active sites of caspases. Although the selectivity of caspases for short

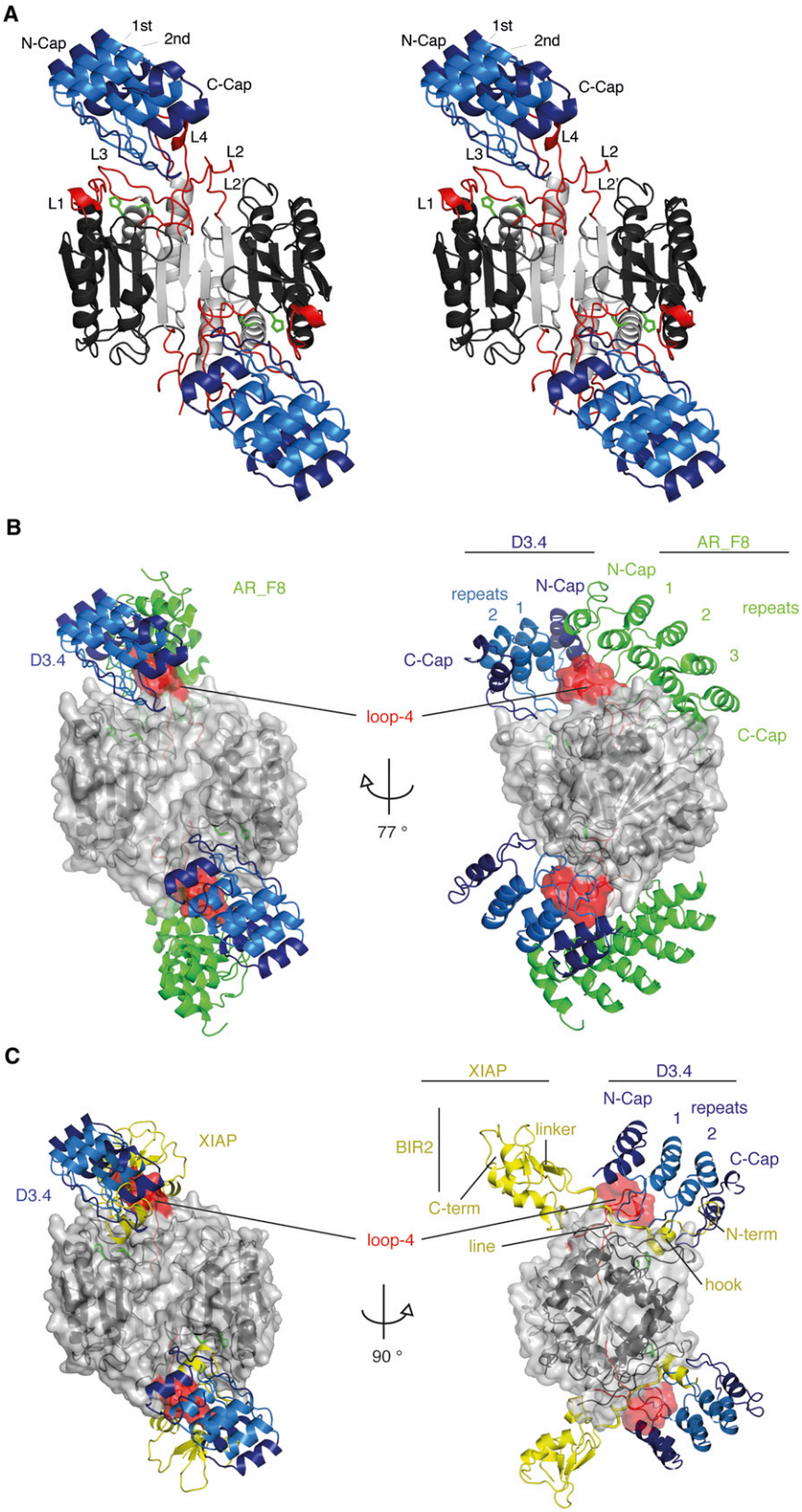

Figure 4. Structures of Caspase-3 in Complex with Different Inhibitors

(A) Stereo view of the caspase-3/D3.4 complex structure as a ribbon cartoon. The two chains of caspase-3 are colored in dark (p17) and light gray (p12). The active site L1, L2, and L4 loops and the catalytic residues are highlighted in red and green, respectively. D3.4 consists of N- and C-terminal capping repeats (dark blue) and two internal repeats (light blue). D3.4 binds in the active site and interacts mainly with loop-4 of caspase-3.

(B) The superposition of the caspase-2 specific DARPin AR_F8 (green, 2P2C) on the caspase-3/D3.4 structure is shown in two different views. Caspases are shown as a gray surface. Darpins D3.4 (blue) and AR_F8 (green) recognize the active site loop-4 (red), albeit from different sides.

(C) The caspase-3/XIAP structure (yellow, 1I3O) was superimposed on the caspase-3/D3.4 structure. The C-terminal BIR2 domain of XIAP binds outside the active side cleft and inhibits the enzyme with the N-terminal tail.

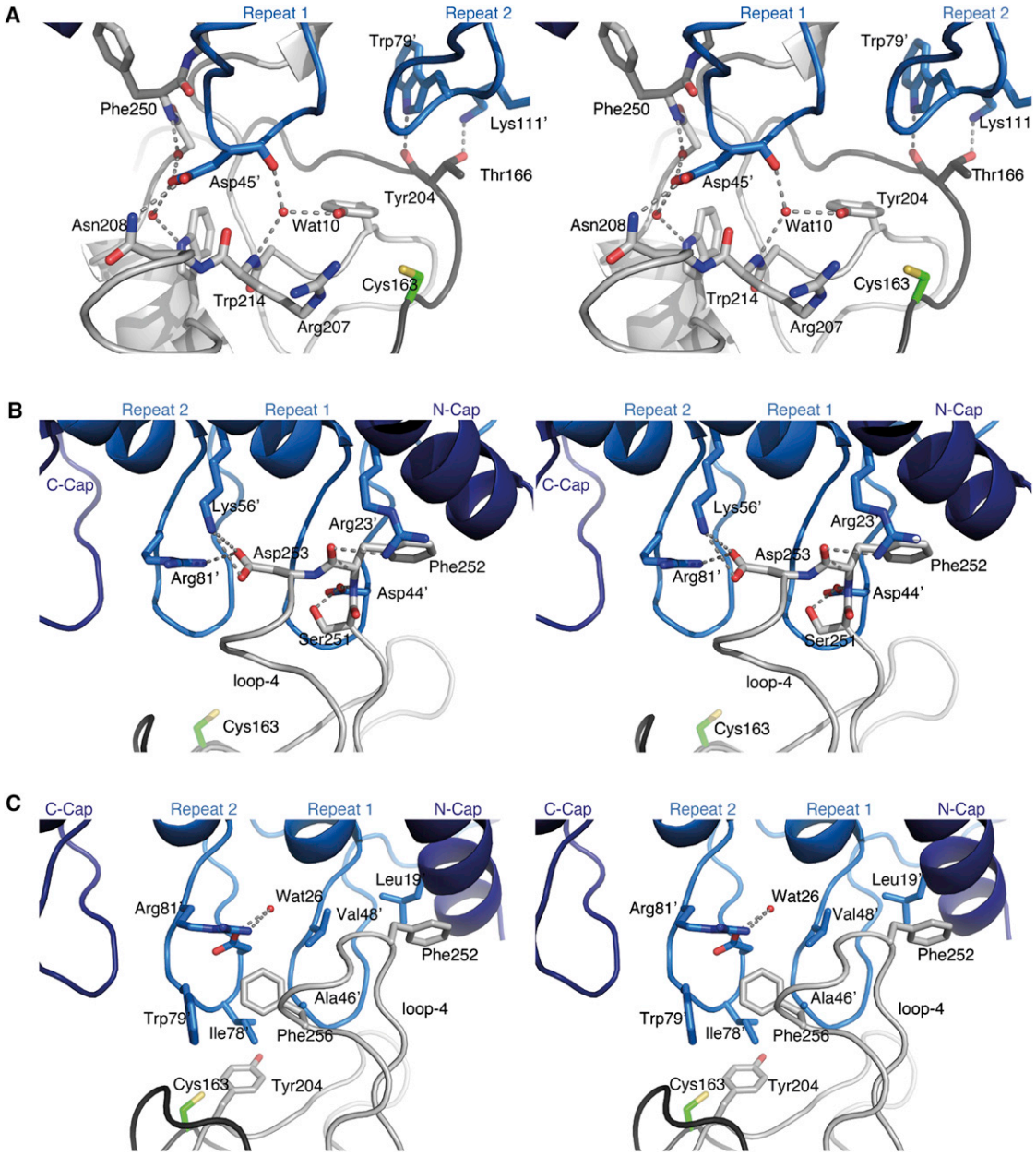

Figure 5. Binding Interface of Caspase-3 with D3.4

Close-up views of the caspase-3/D3.4 interaction in stereo. D3.4 (blue) interacts with caspase-3 (p17, dark gray; p12, light gray) via hydrogen bonds (dotted lines) and hydrophobic interactions. Amino acids from the DARPin are labeled by an additional '. The active site cysteine is shown in green.

(A) Active site standard view: Asp45' forms several hydrogen bonds in the S4 pocket of caspase-3. Thr166, which is located close to the active site Cys163, forms two hydrogen bonds with the second repeat of D3.4.

(B and C) View from the backside of loop-4: The concave site of D3.4 recognizes the tip of loop-4 by several hydrogen bonds (B). The hydrophobic interactions in the interface between caspase-3 and D3.4. Phe256 from caspase-3 binds into a hydrophobic pocket of D3.4 and forms T-stacking interactions with Trp79' (C). See also Figure S5.

peptide inhibitors that differ in the P4 positions is well established (Thornberry et al., 1997), their selectivity is often insufficient considering the different amounts of active caspases in cells undergoing apoptosis (Berger et al., 2006). In 2007, Schweizer et al. published the first truly specific caspase inhibitor (AR_F8) that inhibits caspase-2 with an allosteric mechanism by interacting with loop-4 (Schweizer et al., 2007).

Using the same technology (Binz et al., 2003), we identified four caspase-3 DARPins, two of which specifically inhibited the enzyme. Kinetic analysis characterized D3.4 and D3.8 as purely competitive inhibitors, which is in agreement with the structural data. In the caspase-3/D3.4 structure, the DARPin occupies the active site pocket and recognizes loop-4 of caspase-3. The caspase-2-directed DARPin AR_F8 also recognizes loop-4,

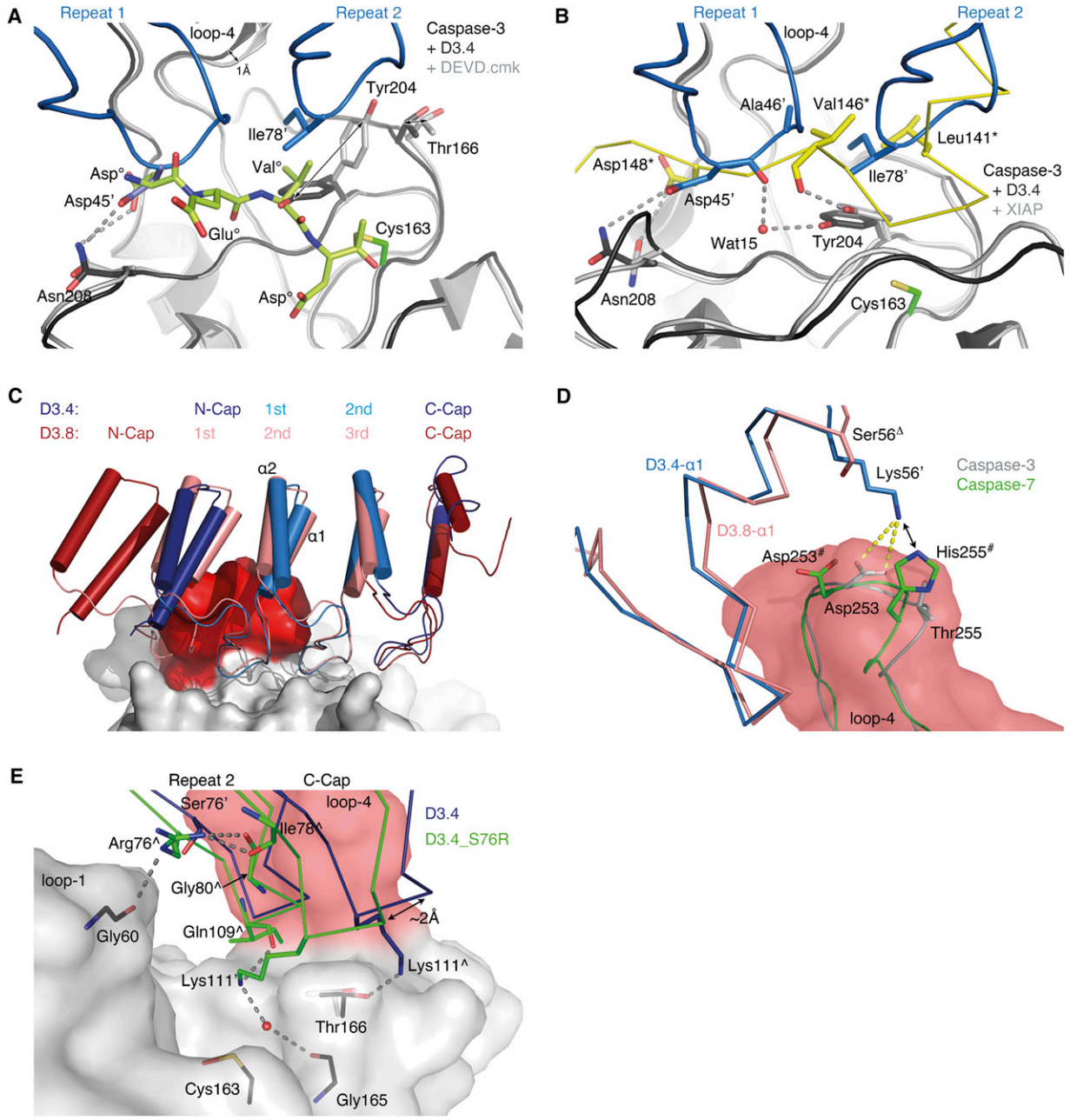

Figure 6. Structural Comparison of Caspase-3 Inhibitors

With the exception of caspase-3, the labels of all amino acids contain unique identifiers: D3.4 (’), DEVD (°), XIAP (*), D3.4_S76R (^), D3.8 ($^{\Delta}$), and caspase-7 ($^{\#}$).

(A) Superposition of caspase-3/z-DEVD-fmk (light green and gray, 2DKO) on the caspase-3/D3.4 structure (dark gray and blue). Tyr204 is rotated by approximately 120° in the DARPin bound structure. As a consequence of this rotation Thr166 is shifted away from the active site. Movements are indicated by black arrows.

(B) Superposition of caspase-3/XIAP (gray and yellow, 1I3O) on the caspase-3/D3.4 structure (dark gray and blue) indicating a similar orientation of Tyr204 in a subsite S2-blocking position.

(C) The D3.8 model (dark red and salmon represent the capping and internal repeats, respectively) superimposed on D3.4 (dark and light blue) with numbered α helices in repeat 2 (D3.8) and 1 (D3.4), respectively. Caspase-3 is shown as a gray surface with loop-4 highlighted in red.

(D) Close-up view of the modeled interaction between either D3.4 (blue) or D3.8 (salmon) and either caspase-3 (gray) or caspase-7 (green). Shown are the α helices 1 of the first internal repeat of D3.4 and the second internal repeat of the D3.8 model. In the caspase-3/D3.4 complex Lys56’ forms a salt bridge with Asp253. In caspase-7, this position is occupied by His255$^{\#}$. In D3.8 Ser56$^{\Delta}$ cannot form the salt bridge with caspase-3 and does not exert repulsive interactions with His255$^{\#}$ in caspase-7.

(E) Superposition of the caspase-3/D3.4 on the caspase-3/D3.4_S76R structure. Caspase-3 is shown as a gray surface with loop-4 colored in red, whereas D3.4 and D3.4_S76R are shown as dark blue and green Cα-traces. Interacting side chains are highlighted. Hydrogen bonds are indicated as gray dotted lines. In the caspase-3/D3.4_S76R structure the side chain of Arg76^, Ile78^, and Lys111^ form hydrogen bonds that are not seen in the parent structure (Table 3) and cause a shift of the C-cap.

Table 3. Hydrogen Bonds in the Caspase-3/D3.4 Interface

DARPin	Distance	Caspase-3
D:ARG 23 [NH1]	3.19	C:PHE 252 [O][a]
D:ASP 44 [OD2]	2.69	C:SER 251 [OG][a]
D:ASP 44 [OD2]	2.97	C:PHE 252 [N][a]
D:ASP 45 [OD1]	3.1	C:ASN 208 [ND2][b]
D:ASP 45 [O]	2.5/2.8	C:Wat 10 - TYR 204 [OH][b]
D:ASP 45 [OD2]	2.6/2.7	C:Wat 12 - PHE 250 [N][a]
D:ASP 45 [OD2]	2.6/2.9	C:Wat 11 - TRP 214 [NE1][b]
D:LYS 56 [NZ]	3.38	C:ASP 253 [OD1][a]
D:LYS 56 [NZ]	–	C:ASP 253 [OD2][a]
D:TRP 79 [NE1]	2.87	C:THR 166 [O][a]
D:ARG 81 [NH2]	2.79	C:ASP 253 [OD2][a]
D:LYS 111 [NZ]	3.75	C:GLU 167 [OE2][a]
D:LYS 111 [NZ][c]	2.68	C:THR 166 [OG1][a]
D3.4_S76R		
D:ARG 76 [NE]	3.3	C:GLY 60 [O][a]
D:LYS 111 [NZ]	2.7/3.2	C:Wat - GLY 165 [O][a]

[a]Caspase residues, not involved in subsite formation.
[b]Caspase residues, forming substrate binding pockets S4–S1.
[c]Not present in D3.4_S76R.

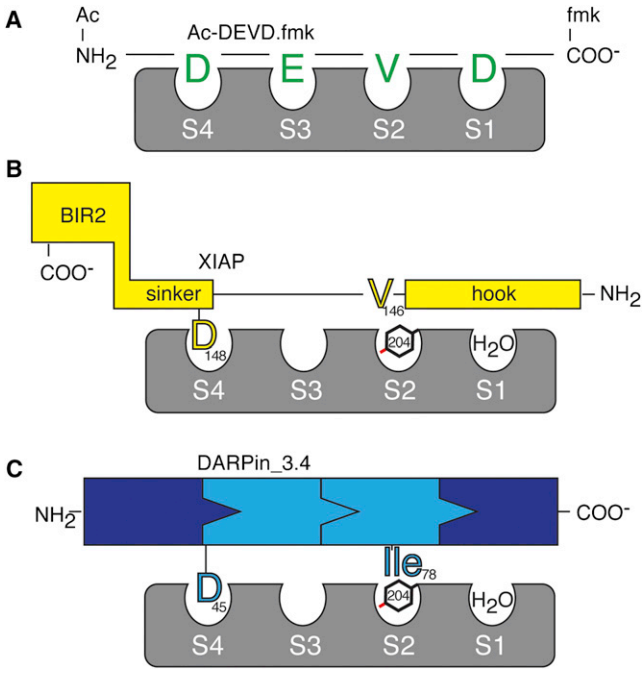

Figure 7. Schematic Caspase-3 Inhibition

(A) The peptide inhibitor Ac-DEVD-fmk occupies four substrate binding pockets of caspase-3 (S1–S4).

(B) The BIR2 domain of XIAP occupies the S4 pocket of caspase-3 with Asp146 and Val146 keeps Tyr204 at a position, which blocks the S2 pocket. S1 is filled with water molecules. Compared to Ac-DEVD-fmk the XIAP main chain runs in the opposite direction.

(C) D3.4 uses a caspase-3 inhibition mechanism that shares features of XIAP and Ac-DEVD-fmk. The S4 pocket is also occupied (Asp45), Ile78 keeps Tyr204 in a locked conformation and the S1 pocket is filled with water, but the D3.4 main chain runs in the same direction like in Ac-DEVD-fmk.

however from a different direction than the caspase-3-directed DARPin D3.4. Its kinetic characterization using the specific velocity plot demonstrated a mixed type inhibition with a significant part of uncompetitive inhibition. The different inhibition modes of D3.4 and AR_F8 can be explained by the different epitopes on the caspases. AR_F8 recognizes caspase-2 from the backside of loop-4 and stabilizes a distinct conformation, which is not able to bind the substrate, whereas D3.4 binds straight into the active site of caspase-3. Our analysis further showed that D3.4 prevents substrates from accessing the catalytic Cys163 and leaves the conformation of loop-4 almost undisturbed when compared to the caspase-3 inhibitor structure.

Another finding is the superior inhibition of caspase-3 by the closely related D3.8, which inhibits caspase-3 even better than D3.4. DARPin molecules D3.6 and D3.13 bind caspase-3 but do not inhibit hydrolysis and were thus not further analyzed. D3.4 does not inhibit the closely related caspase-7 but from the data given in Figure 2 the IC_{50} value for the inhibition of caspase-7 by D3.8 can be estimated to be in the lower micro-molar range. This residual activity is probably resulting from the replacement of Lys56 in D3.4 to Ser56 in D3.8. Lys56 in D3.4 forms a salt bridge with Asp253 from caspase-3 and at the same time could enforce a repulsive effect to His255 from caspase-7 to ensure specificity for caspase-3. The model of the less specific D3.8 does not show this repulsion at caspase-7, which could explain the slight binding ability of D3.8 for caspase-7. Thus, even inhibitors with significantly extended interaction surfaces compared to tetrapeptide inhibitors can recognize closely related caspases, albeit with affinity constants that differ by at least three orders of magnitude.

Our inhibition studies using PARP-1 as a caspase substrate revealed that the selected DARPins (D3.4, D3.4_S76R and D3.8) inhibit PARP-1-cleavage by caspase-3 completely using a 50-fold molar excess. In contrast, caspase-7 cleavage is not influenced even with a 100-fold excess of D3.4, D3.4_S76R, or D3.8, respectively.

Our data suggest that D3.4 and D3.8 bind to the same caspase-3 epitope because residues that seem to be crucial for the recognition of this epitope, such as Asp45, Ala46, Val48, Ile78, Trp79, and Arg81, are conserved in both molecules. The crystal structure revealed that D3.4 recognizes caspase-3 by a set of specific hydrogen bonds, salt bridges and hydrophobic contacts (Table 3). Particularly interesting are the interactions formed by Asp45, which occupies the S4 pocket. So far all structurally characterized caspase-3 specific peptide inhibitors harbor an aspartic acid that occupies this pocket (Figure 7). Although the hydrogen bonding networks are different in the structures of caspase-3 in complex with D3.4, z-DEVD-cmk or XIAP, the positive electrostatic potential explains the preference for a small and negatively charged hydrogen bonding partner like aspartate. Further similarities between the complex structures of caspase-3 with D3.4 and XIAP are seen for Tyr204 (Figure 7). In both structures the Tyr204 side chain points toward Arg341, placing the phenyl ring at van der Waals distance to Cys163-Sγ. On the opposite side the Tyr204 phenyl ring rests against a hydrophobic core, which is composed of caspase-3 residues Leu168 and Phe256 and the side chains of Ala46 and Ile78 from D3.4 or Leu141 and Val146 from XIAP. D3.4 and XIAP are

both lacking an aspartic acid that could occupy the S1 pocket of caspase-3, which consequently is filled by water molecules. The same conformation of Tyr204 is also seen in several other structures of caspase-3 in complex with low molecular weight inhibitors that are lacking a P1 aspartate (Agniswamy et al., 2009; Ganesan et al., 2011) as well as in unliganded caspase-3 (Ni et al., 2003). Conversely, this conformation is different from structures with classical tetrapeptide inhibitors, where the Tyr204 side chain rests against the side chain of Thr166 (Ganesan et al., 2006).

The main chains of the small peptide inhibitor z-DEVD.cmk and D3.4 run antiparallel to caspase-3 residues 204–208. The S4 pocket of caspase-3 is occupied by Asp1 and Asp45 of z-DEVD.cmk and D3.4, respectively. In contrast to that the main chain of XIAP runs parallel to caspase-3 with Val146 and Asp148 binding into the S2- and the S4 pocket, respectively. Although the main chains of D3.4 and XIAP run in opposite directions, both inhibitors use very similar interactions to inhibit caspase-3 (Figure 7). Thus, the comparison of the caspase-3/D3.4 crystal structure with the caspase-3/XIAP crystal structure provides an interesting example for the molecular mimicry of natural and designed caspase-3 inhibitors.

In summary, our study presents the selection and characterization of caspase-3-directed DARPin inhibitors with implications for specificity and inhibition mechanism. The selected DARPins D3.4 and D3.8 are pure competitive inhibitors. D3.4 and the improved variant D3.4_S76R are the first truly specific caspase-3 inhibitors and do not bind caspase-7, a close caspase-3 paralog, or any other human caspase. Such highly specific binders/inhibitors are a prerequisite for the analysis of the function of any enzyme involved in signaling pathways. In the particular case of caspase-3 and its role in apoptotic signaling, D3.4_S76R is the best molecule for such an analysis. Remarkably D3.4 inhibits caspase-3 with a similar mechanism compared to XIAP, the natural caspase-3 inhibitor that also inhibits caspase-7. It has previously been postulated that specificity is achieved by two key factors, allosteric regulation and scanning of large volumes of conformational space (Salvesen and Riedl, 2007). While the second aspect holds true, we demonstrate here that specificity can be achieved even when the conserved substrate binding pockets are targeted, provided this is combined with specific surface recognition of non-subsite residues, which are unique to the targeted protein.

EXPERIMENTAL PROCEDURES

DARPin Selection with Ribosome Display

We performed four rounds of ribosome display to enrich caspase-3 specific binders based on a NI3C and NI2C library as described before (Binz et al., 2004; Zahnd et al., 2007). Prior to each selection the DARPin-ribosome-mRNA complex was incubated with the closest homologous of caspase-3 (caspase-6 and -7) and streptavidin for 30 min at 4°C to avoid selection of unspecific DARPins. Biotinylated caspase-3 was immobilized on magnetic particles (Dynabeads, Invitrogen) for solution panning. DARPin selection was performed in the absence of a caspase-3 inhibitor. The DARPin-ribosome-mRNA complex was incubated with 20 μl of beads for 30 min at 4°C in a tube that was previously blocked with TBST-BSA (50 mM Tris-HCl pH 7.4, 150 mM sodium chloride, 0.05% Tween-20, 0.1% BSA). The incubation was followed by four washing cycles in 50 mM Tris-acetate pH 7.4, 150 mM sodium chloride, 50 mM magnesium acetate, and 0.05% Tween-20. The RNA was eluted in 50 mM Tris-acetate pH 7.4, 150 mM sodium chloride, and 25 mM EDTA and transcribed into DNA for amplification. In rounds three and four, we added a 1000-fold excess of unbiotinylated caspase-3 for 10 min during the selection to favor the enrichment of DARPins with slow k_{off} rates. After four rounds of selection, we cloned the DARPin library in a pQE30 vector (-QIAGEN), transformed competent XL1 blue cells (Stratagene), and continued with crude cell extract ELISA.

Crude Cell Extract ELISA

Single colonies each containing one DARPin clone of the selected library were picked and inoculated in 0.9 ml auto-inducing media 5052 (Studier, 2005) containing deep 96-well plates (Abgene, UK). The cells were grown over night at 37°C while shaking at 300 rpm in a shaker (TH15, Edmund Bühler GmbH). Then 200 μl of each well were transferred into a sterile 96-well plate (449824, Nunc) as a backup for further protein expression and plasmid preparation. The remaining 700 μl of cell-suspension was harvested by centrifugation and the cell pellet was lysed with 50 μl B-PER II (Pierce, 78260) per well for 30 min shaking at room temperature. The lysed cells were resuspended by adding 950 μl PBS, pH 7.3, and cell debris were removed by centrifugation (20 min, 4500 rpm at 4°C) in a tabletop centrifuge (Eppendorf). We now took 20 μl of the supernatant of four 96 well plates and transferred it to one 384-well ELISA plate (Nunc, 464718). This plate was previously coated with 20 μl of a 22 nM neutravidin solution (Pierce, 31000) and biotinylated caspase-3, followed by extensive washing. After 1 hr of incubation at room temperature and three washing cycles, the plate was incubated with mouse anti-RGS-H_4 antibody (QIAGEN, 34650) at a dilution of 1:2000 in PBS 1% BSA. After adding the secondary antibody (goat-α-mouse IgG alkaline phosphatase conjugate, Sigma, A3562) and four washing steps the amount of bound DARPin was quantified by adding the substrate buffer (3 mM di-sodium 4-nitrophenyl phosphate, 50 mM sodium bicarbonate, 50 mM magnesium chloride). The optical density (OD) was measured at 405 nm using a multiwell plate reader (Infinite M1000, Tecan).

Expression, Purification, and Biotinylation of Proteins

All DARPins were expressed in auto-inducing media (Studier, 2005) or lysogeny broth media (Binz et al., 2003). The expressed DARPin was purified by IMAC using a self-made gravity column (Supelco, 57024) containing 0.5 ml bead volume of Ni^{2+}-NTA agarose (QIAGEN, 30210). The DARPins were eluted in PBS complemented with 200 mM imidazole. The imidazole was removed with a PD-10 desalting column (GE Helthcare, 17-0435-01). We added sodium azide to a final concentration of 0.03% to prevent growth of bacteria and fungi. The DARPin solutions were stored at 4°C. Caspase-1 to caspase-9 were expressed and purified as described elsewhere (Roschitzki-Voser et al., 2012). Expression plasmids for caspase-6, -7, and -9 have been obtained from Dr. Guy Salvesen, the Burnham Institute, La Jolla, CA, USA (Denault and Salvesen, 2003).

For chemical biotinylation of caspases, we used the linker EZ-Link Sulfo-NHS-LC-LC-Biotin (Pierce, 21338), containing a reactive group, a 3.05-nm long linker, and a biotin moiety. After purification, 1 ml of 10 μM caspase in PBS, pH 7.3 was incubated with a 7-fold molar excess (1 ml of a 70 μM solution) of biotin on ice for 30 min. The reaction was quenched by adding 10 μl of 5 M Tris-HCl, pH 7.5. The biotinylated protein was purified by size exclusion chromatography, using a Superdex 200 10/300 GL (GE Healthcare) in PBS at 4°C. Fractions containing biotinylated caspase were pooled and frozen in liquid nitrogen after adding sucrose to a final concentration of 10%.

Crystallization

The caspase/DARPin complexes were formed by incubating caspase-3 with a 2-fold molar excess of each DARPin for 10 min on ice. The complex was purified by size exclusion chromatography (Superdex 200 HR 10/30, Amersham Pharmacia, Sweden) in 50 mM Tris-HCl, pH 8.0 (4°C), 50 mM sodium chloride. Fractions containing caspase/DARPin were concentrated to 5 mg/ml and 10 mg/ml for D3.4 and D3.4_S76R, respectively, using an ultrafiltration device with a molecular weight limit of 15 kDa (Amicon Ultra, Millipore).

Crystals were grown at room temperature using the vapor-diffusion method. Two microliters of concentrated protein solution were mixed with 1 μl of reservoir solution containing 100 mM HEPES, pH 7.3, 70% (v/v) 2-methyl-2,4-pentanediol. Crystallization plates were stored at 20°C. Crystals appeared within 24 hr.

Data Collection, Structure Determination, and Refinement

For X-ray diffraction analysis, crystals were flash-frozen in liquid nitrogen and data were collected (100 K) at beamline X06SA (Swiss Light Source, Villigen, Switzerland). No cryoprotectant was necessary for data collection. The beamline was equipped with a Pilatus 6M fast readout pixel detector (Dectris, Switzerland). The program XDS was used for data processing and data were scaled with XSCALE (Kabsch, 2010; Potterton et al., 2003). Both complexes crystallized in space group $P3_121$. Unit cell dimensions are listed in Table 2. The structures were solved by molecular replacement with the program PHASER (McCoy et al., 2007) using a high-resolution structure of caspase-3 (2DKO; Ganesan et al., 2006) and a model of the N2C DARPin, which was generated by homology modeling (MODELER 9v8; Eswar et al., 2007) using the N3C DARPin E3_5 (1MJ0; Kohl et al., 2003) as a template. The crystals have a solvent content of 59% (Matthews coefficient of 3.0 $Å^3$/Da) (Collaborative Computational Project, Number 4, 1994) with one (p12, p17, D3.4)$_2$ complex in the asymmetric unit. Alternating rounds of manual model building using COOT (Emsley et al., 2010) and restrained refinement using REFMAC version 5.5.01.09 (Murshudov et al., 1997) yielded R_f/R_{free} values of 0.185/0.217 for the caspase-3/D3.4 and 0.174/0.214 for the caspase-3/D3.4_S76R complex. Data collection and structure refinement statistics are listed in Table 2. Structures were superimposed using COOT (Emsley et al., 2010) and figures were prepared using PyMOL (Schrodinger, 2010).

Site-Directed Mutagenesis

We used the QuikChange Site Directed Mutageneis Kit (Stratagene) to incorporate mutations in the DARPin sequence. The following primers were used to introduce the Ser76Arg mutation in D3.4: 5′-GGT GCT GAC GTT AAC GCT CGT GAC ATT TGG GGT CGT ACT-3′ (fwd) and 5′-AGT ACG ACC CCA AAT GTC ACG AGC GTT AAC GTC AGC ACC-3′ (rev). The underlined codons indicate the mutation.

Surface Plasmon Resonance Analysis

For SPR experiments we used the Proteon XPR36™ (Biorad Laboratories) and a NLC sensor chip (Biorad Laboratories). Sterile filtered PBS, pH 7.3, and 0.005% Tween-20 were used as the standard buffer for all coating and kinetic analysis steps. A 5-nM solution of biotinylated, fully processed caspase was coated in the absence of caspase inhibitors on the sensor chip at a flow rate of 30 μl per minute. The coating procedure was stopped when 1000 relative units were immobilized on the chip. Dilution series of DARPins were pipetted in 96-deep well plates (Biorad, 176-6023), which were sealed to prevent evaporation and contamination with dust particles. Starting with the lowest concentration we measured the binding of DARPins at 0, 0.176, 0.52, 1.58, 4.47, 14.2, 42.6, and 128 nM concentrations. All experiments were performed at 20°C. Flow rates of 100 μl per minute, association times of 3 min and dissociation times of 20 min were used. Data were recorded and kinetic binding data were determined with the ProteOn Manager 2.1.1 software (Biorad) using the heterogeneous ligand model (Bravman et al., 2006).

Caspase Activity Measurements

Specific inhibition of caspase-1 to caspase-9 was measured using peptide substrates from Peptide Institute (Osaka, Japan). We used Ac-DEVD-amc for caspase-3, -6, -7, and -8; Ac-WEHD-amc for caspase-1, -4, and -5; Ac-VDVAD-amc for caspase-2; and Ac-LEHD-amc for caspase-9. Enzyme and substrate concentrations in the assay were as follows: caspase-1 (10 nM enzyme; 150 μM substrate), caspase-2 (25 nM; 150 μM), caspase-3 (0.5 nM; 150 μM), caspase-4 (200 nM; 600 μM), caspase-5 (10 nM; 150 μM), caspase-6 (10 nM; 600 μM), caspase-7 (2 nM, 400 μM), caspase-8 (10 nM; 150 μM), and caspase-9 (25 nM, 600 μM) considering all caspases as heterotetramers. DARPins were added assuming that one DARPin binds to every caspase active site. The following assay buffers were used: caspase-2, 100 mM MES, pH 6.5, 10% PEG600 (w/v), 0.1% CHAPS (w/v), 10 mM DTT; caspase-9, 50 mM Tris-HCl, pH 7.5, 10% sucrose (w/v), 1.3 M sodium citrate; all other caspases, 20 mM PIPES, pH 6.5, 10% sucrose (w/v), 0.1% CHAPS (w/v), 10 mM DTT, 150 mM sodium chloride, and 1 mM EDTA. AMC release was monitored by measuring the fluorescent excitation and emission wavelengths of 360 nm and 465 nm, respectively, using an Infinite M-1000 spectrofluorometer (Tecan).

Specific Velocity Plot

Inhibition mechanism and K_i values of DARPins D3.4, D3.8, and D3.4_S76R have been determined using the specific velocity plot (Baici, 1981). The concentration of caspase-3 was determined by active site titration as described previously (Stennicke et al., 2000). The caspases inhibitor Ac-DEVD-cmk (0 to 7.6 nM), caspase-3 (0.5 nM), and the substrate Ac-DEVD-amc (100 μM) were prepared in activity buffer containing no DTT (20 mM PIPES, pH 6.5, 10% sucrose [w/v], 0.1% CHAPS [w/v], 150 mM sodium chloride, 1 mM EDTA). Concentrations of DARPins were determined using amino acid analysis at the Functional Genomic Center (Zürich, Switzerland). The initial velocities of substrate hydrolysis with 0.5 nM caspase-3 have been measured at different DARPin concentrations (D3.4, 8–32 nM; D3.4_S76R, 4–10 nM; D3.8, 2–8 nM) and substrate concentration between 0.2 and 0.8 times K_m (K_m = 24.7 ± 1.8 μM). Graphical analysis of the velocity plot was done with Prism5 (GraphPad Software). The inhibitor titration has been performed using 0.5 nM caspase-3, different DARPin concentrations (D3.4, 0–1,000 nM; D3.4_S76R, 0–1,000 nM; D3.8, 0–100 nM), and 24 μM substrate. To determine K_i values of DARPins initial velocities were fitted to the tight binding inhibition equation as described previously (Szedlacsek et al., 1988).

PARP-1 Inhibition and Western Blot Analysis

A 0.18-μM solution of PARP-1 in 50 mM Tris-HCl, pH 7.5, 150 mM sodium chloride was mixed with either 40 nM caspase-3 or 150 nM caspase-7 and the corresponding DARPin (10- to 100-fold excess per active site) as indicated in Figure 2. The mixture was incubated for 20 min at room temperature in 50 mM Tris-HCl pH 7.5, 150 mM sodium chloride, and 0.5 mM DTT, and stopped by adding SDS sample buffer (95°C for 5 min). The samples were subjected to 12% SDS-PAGE under reducing conditions and transferred to a nitrocellulose membrane (iBlot, Invitrogen). The membrane was blocked in high-TBS (50 mM Tris-HCl, pH 7.5, 500 mM sodium chloride) containing 5% (w/v) nonfat dry milk for 1 hr at room temperature. The primary PARP antibody (Cell Signaling, 9542) was incubated with the membrane at a dilution of 1:1000 in high-TBS-T (50 mM Tris-HCl, pH 7.5, 500 mM sodium chloride, 0.1% Tween-20) at 4°C overnight. After intensive washing in high-TBS-T, we incubated the membrane with anti-rabbit HRP conjugated antibody (Cell Signaling, 7074) for 1 hr at room temperature in TBS (50 mM Tris-HCl, pH 7.5, 150 mM sodium chloride). Protein bands were visualized by chemiluminescence using the SuperSignal West Pico Chemiluminescent Substrate (Pierce) in combination with a Fuji Las 3000 camera.

Modeling of D3.8

Based on the kinetic data and sequence alignments, we hypothesized that D3.8 binds to the same epitope as D3.4. Therefore, we generated a model of D3.8 in complex with caspase-3. The N3C DARPin E3_5 (1MJ0; Kohl et al., 2003) was used as a template to calculate a homology model of D3.8 using the program MODELER 9v8 (Eswar et al., 2007). The model of D3.8 was then superimposed on D3.4 in the complex structure according to the sequence alignment shown in Figure 1.

ACCESSION NUMBERS

The Protein Data Bank (PDB) accession numbers for the coordinates and structure factors of caspase-3 in complex with DARPin D3.4 and with DARPin D3.4_S76R, respectively, reported in this paper are 2XZD and 2Y0B.

SUPPLEMENTAL INFORMATION

Supplemental Information includes five figures and can be found with this article online at http://dx.doi.org/10.1016/j.str.2012.12.011.

ACKNOWLEDGMENTS

This work was supported by Swiss National Science Foundation grant 310030-122342 to M.G.G. We gratefully acknowledge the Salvesen laboratory for the expression plasmid of caspase-6 and -7 as well as Prof. M. Hottiger (University Zürich, Switzerland) for providing a sample of PARP-1 for the caspase inhibition studies. We acknowledge Prof. A. Baici for discussion

and advice on the evaluation of our kinetic experiments. Crystallographic data collection was performed at the Swiss Light Source (Paul Scherrer Institute, Villigen, Switzerland). SPR data were measured at the Functional Genomics Center Zürich. T.S. is a member of the Molecular Life Science Ph.D. program at the ETH/University of Zürich. J.B. and A.F. are members of the Biomolecular Structure Ph.D. program at the ETH/University of Zürich.

Received: October 18, 2012
Revised: December 3, 2012
Accepted: December 14, 2012
Published: January 17, 2013

REFERENCES

Agniswamy, J., Fang, B., and Weber, I.T. (2009). Conformational similarity in the activation of caspase-3 and -7 revealed by the unliganded and inhibited structures of caspase-7. Apoptosis *14*, 1135–1144.

Amstutz, P., Binz, H.K., Parizek, P., Stumpp, M.T., Kohl, A., Grütter, M.G., Forrer, P., and Plückthun, A. (2005). Intracellular kinase inhibitors selected from combinatorial libraries of designed ankyrin repeat proteins. J. Biol. Chem. *280*, 24715–24722.

Baici, A. (1981). The specific velocity plot. A graphical method for determining inhibition parameters for both linear and hyperbolic enzyme inhibitors. Eur. J. Biochem. *119*, 9–14.

Berger, A.B., Sexton, K.B., and Bogyo, M. (2006). Commonly used caspase inhibitors designed based on substrate specificity profiles lack selectivity. Cell Res. *16*, 961–963.

Binz, H.K., Stumpp, M.T., Forrer, P., Amstutz, P., and Plückthun, A. (2003). Designing repeat proteins: well-expressed, soluble and stable proteins from combinatorial libraries of consensus ankyrin repeat proteins. J. Mol. Biol. *332*, 489–503.

Binz, H.K., Amstutz, P., Kohl, A., Stumpp, M.T., Briand, C., Forrer, P., Grütter, M.G., and Plückthun, A. (2004). High-affinity binders selected from designed ankyrin repeat protein libraries. Nat. Biotechnol. *22*, 575–582.

Binz, H.K., Amstutz, P., and Plückthun, A. (2005). Engineering novel binding proteins from nonimmunoglobulin domains. Nat. Biotechnol. *23*, 1257–1268.

Boatright, K.M., Renatus, M., Scott, F.L., Sperandio, S., Shin, H., Pedersen, I.M., Ricci, J.E., Edris, W.A., Sutherlin, D.P., Green, D.R., and Salvesen, G.S. (2003). A unified model for apical caspase activation. Mol. Cell *11*, 529–541.

Bravman, T., Bronner, V., Lavie, K., Notcovich, A., Papalia, G.A., and Myszka, D.G. (2006). Exploring "one-shot" kinetics and small molecule analysis using the ProteOn XPR36 array biosensor. Anal. Biochem. *358*, 281–288.

Collaborative Computational Project, Number 4 (1994). The CCP4 suite: programs for protein crystallography. Acta Crystallogr. D Biol. Crystallogr. *50*, 760–763.

Denault, J.B., and Salvesen, G.S. (2003). Expression, purification, and characterization of caspases. Curr Protoc Protein Sci., Chapter 21, Unit 21 13.

Deveraux, Q.L., Takahashi, R., Salvesen, G.S., and Reed, J.C. (1997). X-linked IAP is a direct inhibitor of cell-death proteases. Nature *388*, 300–304.

Emsley, P., Lohkamp, B., Scott, W.G., and Cowtan, K. (2010). Features and development of Coot. Acta Crystallogr. D Biol. Crystallogr. *66*, 486–501.

Eswar, N., Webb, B., Marti-Renom, M.A., Madhusudhan, M.S., Eramian, D., Shen, M.Y., Pieper, U., and Sali, A. (2007). Comparative protein structure modeling using MODELLER. Curr Protoc Protein Sci., Chapter 2, Unit 2 9.

Fuentes-Prior, P., and Salvesen, G.S. (2004). The protein structures that shape caspase activity, specificity, activation and inhibition. Biochem. J. *384*, 201–232.

Ganesan, R., Mittl, P.R., Jelakovic, S., and Grütter, M.G. (2006). Extended substrate recognition in caspase-3 revealed by high resolution X-ray structure analysis. J. Mol. Biol. *359*, 1378–1388.

Ganesan, R., Jelakovic, S., Mittl, P.R., Caflisch, A., and Grütter, M.G. (2011). In silico identification and crystal structure validation of caspase-3 inhibitors without a P1 aspartic acid moiety. Acta Crystallogr. Sect. F Struct. Biol. Cryst. Commun. *67*, 842–850.

Grütter, M.G. (2000). Caspases: key players in programmed cell death. Curr. Opin. Struct. Biol. *10*, 649–655.

Kabsch, W. (2010). Integration, scaling, space-group assignment and post-refinement. Acta Crystallogr. D Biol. Crystallogr. *66*, 133–144.

Kohl, A., Binz, H.K., Forrer, P., Stumpp, M.T., Plückthun, A., and Grütter, M.G. (2003). Designed to be stable: crystal structure of a consensus ankyrin repeat protein. Proc. Natl. Acad. Sci. USA *100*, 1700–1705.

Lazebnik, Y.A., Kaufmann, S.H., Desnoyers, S., Poirier, G.G., and Earnshaw, W.C. (1994). Cleavage of poly(ADP-ribose) polymerase by a proteinase with properties like ICE. Nature *371*, 346–347.

McCoy, A.J., Grosse-Kunstleve, R.W., Adams, P.D., Winn, M.D., Storoni, L.C., and Read, R.J. (2007). Phaser crystallographic software. J. Appl. Cryst. *40*, 658–674.

McStay, G.P., Salvesen, G.S., and Green, D.R. (2008). Overlapping cleavage motif selectivity of caspases: implications for analysis of apoptotic pathways. Cell Death Differ. *15*, 322–331.

Mittl, P.R.E., Di Marco, S., Krebs, J.F., Bai, X., Karanewsky, D.S., Priestle, J.P., Tomaselli, K.J., and Grütter, M.G. (1997). Structure of recombinant human CPP32 in complex with the tetrapeptide acetyl-Asp-Val-Ala-Asp fluoromethyl ketone. J. Biol. Chem. *272*, 6539–6547.

Morton, T.A., Myszka, D.G., and Chaiken, I.M. (1995). Interpreting complex binding kinetics from optical biosensors: a comparison of analysis by linearization, the integrated rate equation, and numerical integration. Anal. Biochem. *227*, 176–185.

Murshudov, G.N., Vagin, A.A., and Dodson, E.J. (1997). Refinement of macromolecular structures by the maximum-likelihood method. Acta Crystallogr. D Biol. Crystallogr. *53*, 240–255.

Muzio, M., Stockwell, B.R., Stennicke, H.R., Salvesen, G.S., and Dixit, V.M. (1998). An induced proximity model for caspase-8 activation. J. Biol. Chem. *273*, 2926–2930.

Ni, C.Z., Li, C., Wu, J.C., Spada, A.P., and Ely, K.R. (2003). Conformational restrictions in the active site of unliganded human caspase-3. J. Mol. Recognit. *16*, 121–124.

Potterton, E., Briggs, P., Turkenburg, M., and Dodson, E. (2003). A graphical user interface to the CCP4 program suite. Acta Crystallogr. D Biol. Crystallogr. *59*, 1131–1137.

Riedl, S.J., and Shi, Y. (2004). Molecular mechanisms of caspase regulation during apoptosis. Nat. Rev. Mol. Cell Biol. *5*, 897–907.

Riedl, S.J., Renatus, M., Schwarzenbacher, R., Zhou, Q., Sun, C., Fesik, S.W., Liddington, R.C., and Salvesen, G.S. (2001). Structural basis for the inhibition of caspase-3 by XIAP. Cell *104*, 791–800.

Roschitzki-Voser, H., Schroeder, T., Lenherr, E.D., Frölich, F., Schweizer, A., Donepudi, M., Ganesan, R., Mittl, P.R., Baici, A., and Grütter, M.G. (2012). Human caspases in vitro: expression, purification and kinetic characterization. Protein Expr. Purif. *84*, 236–246.

Rotonda, J., Nicholson, D.W., Fazil, K.M., Gallant, M., Gareau, Y., Labelle, M., Peterson, E.P., Rasper, D.M., Ruel, R., Vaillancourt, J.P., et al. (1996). The three-dimensional structure of apopain/CPP32, a key mediator of apoptosis. Nat. Struct. Biol. *3*, 619–625.

Roy, N., Deveraux, Q.L., Takahashi, R., Salvesen, G.S., and Reed, J.C. (1997). The c-IAP-1 and c-IAP-2 proteins are direct inhibitors of specific caspases. EMBO J. *16*, 6914–6925.

Salvesen, G.S., and Riedl, S.J. (2007). Caspase inhibition, specifically. Structure *15*, 513–514.

Schrodinger, LLC (2010). The AxPyMOL Molecular Graphics Plugin for Microsoft PowerPoint, Version 1.0.

Schweizer, A., Roschitzki-Voser, H., Amstutz, P., Briand, C., Gulotti-Georgieva, M., Prenosil, E., Binz, H.K., Capitani, G., Baici, A., Plückthun, A., and Grütter, M.G. (2007). Inhibition of caspase-2 by a designed ankyrin repeat protein: specificity, structure, and inhibition mechanism. Structure *15*, 625–636.

Schweizer, A., Rusert, P., Berlinger, L., Ruprecht, C.R., Mann, A., Corthésy, S., Turville, S.G., Aravantinou, M., Fischer, M., Robbiani, M., et al. (2008).

CD4-specific designed ankyrin repeat proteins are novel potent HIV entry inhibitors with unique characteristics. PLoS Pathog. *4*, e1000109.

Sennhauser, G., Amstutz, P., Briand, C., Storchenegger, O., and Grütter, M.G. (2007). Drug export pathway of multidrug exporter AcrB revealed by DARPin inhibitors. PLoS Biol. *5*, e7.

Steiner, D., Forrer, P., Stumpp, M.T., and Plückthun, A. (2006). Signal sequences directing cotranslational translocation expand the range of proteins amenable to phage display. Nat. Biotechnol. *24*, 823–831.

Stennicke, H.R., Renatus, M., Meldal, M., and Salvesen, G.S. (2000). Internally quenched fluorescent peptide substrates disclose the subsite preferences of human caspases 1, 3, 6, 7 and 8. Biochem. J. *350*, 563–568.

Studier, F.W. (2005). Protein production by auto-induction in high density shaking cultures. Protein Expr. Purif. *41*, 207–234.

Szedlacsek, S.E., Ostafe, V., Serban, M., and Vlad, M.O. (1988). A re-evaluation of the kinetic equations for hyperbolic tight-binding inhibition. Biochem. J. *254*, 311–312.

Thornberry, N.A., Rano, T.A., Peterson, E.P., Rasper, D.M., Timkey, T., Garcia-Calvo, M., Houtzager, V.M., Nordstrom, P.A., Roy, S., Vaillancourt, J.P., et al. (1997). A combinatorial approach defines specificities of members of the caspase family and granzyme B. Functional relationships established for key mediators of apoptosis. J. Biol. Chem. *272*, 17907–17911.

Timmer, J.C., and Salvesen, G.S. (2007). Caspase substrates. Cell Death Differ. *14*, 66–72.

Wyllie, A.H., Kerr, J.F., and Currie, A.R. (1980). Cell death: the significance of apoptosis. Int. Rev. Cytol. *68*, 251–306.

Zahnd, C., Amstutz, P., and Plückthun, A. (2007). Ribosome display: selecting and evolving proteins in vitro that specifically bind to a target. Nat. Methods *4*, 269–279.

Zahnd, C., Kawe, M., Stumpp, M.T., de Pasquale, C., Tamaskovic, R., Nagy-Davidescu, G., Dreier, B., Schibli, R., Binz, H.K., Waibel, R., and Plückthun, A. (2010). Efficient tumor targeting with high-affinity designed ankyrin repeat proteins: effects of affinity and molecular size. Cancer Res. *70*, 1595–1605.